Applied Entomology and Zoology (2022) 57:363–377
https://doi.org/10.1007/s13355-022-00795-5

ORIGINAL RESEARCH PAPER

Photoperiod controls insulin and juvenile hormone signaling pathways via the circadian clock in the bean bug *Riptortus pedestris* (Hemiptera: Alydidae)

Genyu Mano[1] · **Shin G. Goto**[1,2]

Received: 18 June 2022 / Accepted: 5 August 2022 / Published online: 21 August 2022

Abstract
Most multivoltine insects in temperate zones enter diapause in response to short days. The photoperiod is evaluated in these organisms by a photoperiodic time measurement system, which involves the circadian clock, and activates or inactivates endocrine organs or cells to alter their physiological status. Although the physiological mechanisms underlying insect photoperiodism have been extensively studied, the molecular linkage between the circadian clock and endocrine signaling pathways remains unclear. In this study, we evaluated the bean bug *Riptortus pedestris* (F.) (Hemiptera: Alydidae), which enters adult (reproductive) diapause in response to short days. A gene encoding the insulin-like peptide ILP1, which is expressed in the pars intercerebralis in the brain, was upregulated and involved in fecundity under long days. *Ilp1* appeared to function independently of the photoperiodic response controlled by juvenile hormone signaling. *Cyp15*, which encodes an epoxidase crucial for juvenile hormone biosynthesis, was upregulated and involved in ovarian development under long days. RNA interference targeted against the circadian clock gene *per* canceled the *Ilp1* and *Cyp15* suppression and allowed females to be reproductive even under diapause-inducing short days. Thus, the circadian clock may control the photoperiodic response by altering the expression of key elements in two independent endocrine pathways.

Keywords Circadian clock · Diapause · Fecundity · RNA interference · Vitellogenesis

Introduction

Photoperiodism is the ability to respond to photoperiods and enables organisms to coordinate their physiological status with annual changes in their biotic and abiotic environments (Danks 1987; Tauber et al. 1986). The most well-known photoperiodic event among insects is diapause, during which development or reproduction is suppressed or arrested and metabolic activity is extensively reduced. Diapause at the egg, larval (or nymphal), and pupal stages is characterized by developmental arrest or suspension, whereas the central feature of diapause at the adult stage is the cessation of reproduction (Denlinger 2022). For example, adults of the bean bug *Riptortus pedestris* (F.) (Hemiptera: Alydidae) allocate energy resources to the reproductive organs to develop these organs for reproductive activities under summer long-day conditions. By contrast, under autumnal short-day conditions, adults accumulate lipids and suppress reproductive organ development for overwintering (Morita et al. 1999; Numata and Hidaka 1982).

Insects assess day or night length using a photoperiodic time measurement system, which is a function of the circadian clock (Nelson et al. 2009). The circadian clock is a biological time-keeping system that controls organismal rhythms over approximately 24 h and is established by a dozen of circadian clock genes, including *period* (*per*), *mammalian-type cryptochrome* (*cry-m*), *Clock* (*Clk*), *cycle* (*cyc*), *timeless*, *PAR-domain protein 1*, *vrille*, and *clockwork orange* (Patke et al. 2020; Tomioka and Matsumoto 2019). Knockdown or knockout of circadian clock genes disrupts photoperiodic responses in various insect species (Goto and Nagata 2022; Ikeda et al. 2021; Meuti et al. 2015; Mukai and Goto 2016; Tamai et al. 2019; Zhu et al. 2019). For example, knockdown of *per* and *cry-m* induces ovarian development

✉ Shin G. Goto
shingoto@omu.ac.jp

[1] Graduate School of Science, Osaka City University, Osaka 558-8585, Japan

[2] Graduate School of Science, Osaka Metropolitan University, Osaka 558-8585, Japan

even under diapause-inducing short-day conditions in *R. pedestris*. By contrast, knockdown of *cyc* and *Clk* suppressed ovarian development even under diapause-averting long-day conditions (Ikeno et al. 2010, 2011a, b, 2013). Thus, the circadian clock composed of these circadian clock genes may be involved in photoperiodic time measurement (Numata et al. 2015).

Insect diapause is regulated by ecdysteroids, juvenile hormone (JH), diapause hormone, and insulin-like peptides (ILPs). Among them, JH and ILPs play major roles in adult diapause (Denlinger 2022). JH is an acyclic sesquiterpenoid that is synthesized in the endocrine organ, the corpus allatum (CA), and by a series of JH biosynthetic enzymes such as JH acid methyltransferase (JHAMT) and cytochrome P450 15 (CYP15) (Goodman and Cusson 2012). Analysis of the photoperiodic control of the JH titer, JH biosynthesis in the CA, and expression of JH biosynthetic enzymes revealed that inactivation of CA leads to a low JH hemolymph titer to induce adult diapause (Hejníková et al. 2022; de Kort et al. 1982; Larrere et al. 1993; Matsumoto et al. 2013; Okuda et al. 1996; Rankin and Riddiford 1978; Readio et al. 1999). Additionally, in *R. pedestris*, allatectomy suppressed reproduction even under diapause-averting long-day conditions (Morita and Numata 1997). Furthermore, topical application of JH III skipped bisepoxide ($JHSB_3$), the JH of this species, and a JH analog induced expression of *Vitellogenin-1* (*Vg-1*) and the hexameric yolk protein gene *Cyanoprotein-α* (*CP-α*) in the fat body as well as ovarian development (Ando et al. 2020; Hirai et al. 1998; Miura et al. 1998). Thus, JH causally regulates diapause in *R. pedestris*.

Studies of the mosquito *Culex pipiens* provided strong evidence that insulin signaling is also a pivotal component regulating photoperiodic adult diapause (Sim and Denlinger 2008, 2009; Sim et al. 2015). In *Drosophila melanogaster*, insulin signaling, initiated in insulin-producing cells in the brain, controls the insulin cascade in the CA, ultimately leading to ovarian development by stimulating JH biosynthesis (Kubrak et al. 2014; Ojima et al. 2018; Schiesari et al. 2016). Apart from the photoperiodic response, an axis from ILPs to vitellogenin gene expression through JH has been proposed in the red flour beetle *Tribolium castaneum* (Sheng et al. 2011). ILPs are expressed in the dorsocentral part of the brain (pars intercerebralis, PI) in various insect species (Barberà et al. 2019; Broughton et al. 2005; Cuti et al. 2021; Goltzené et al. 1992; Mizoguchi et al. 1987; Riehle et al. 2006; Vafopoulou and Steel 2012; Xu et al. 2015). Surgical removal of the PI disrupted photoperiodic ovarian development, supporting a crucial role for ILPs in insect photoperiodism (Hodková 1976; Hodková and Okuda 2019; Poras 1982; Shiga and Numata 2000).

However, the role of ILPs in *R. pedestris* would be different from these species. Surgical removal of the PI did not affect photoperiodic regulation of ovarian development in *R. pedestris*, although fecundity was affected under long-day conditions (Shimokawa et al. 2008, 2014). Silencing of genes encoding two ILPs, *Ilp1* and *Ilp2*, affected fecundity but not ovarian development (Hasebe and Shiga 2021). Alternatively, ovarian development is regulated by JH (Ando et al. 2020; Morita and Numata 1997). These results suggest that the ILP signaling pathway does not reside upstream of the JH signaling pathway, in contrast to that in *C. pipiens* and *D. melanogaster*, rather these pathways independently regulate photoperiodic responses under the control of the photoperiodic time measurement system in *R. pedestris*. However, the photoperiodic regulation of ILPs, location of ILP-producing cells in the brain, and molecular linkage between the circadian clock and ILP and JH signaling pathways are unclear. Thus, an overall understanding of the molecular mechanisms underlying photoperiodism is lacking.

In this study, we examined the relationship between the ILP and JH signaling pathways in the photoperiodic response. We investigated the photoperiodic and temporal regulation of *Ilp1* and *Ilp2*, location of cells expressing ILP1, and function of ILP1 in the photoperiodic response using RNA interference (RNAi). We also evaluated the molecular linkage between the circadian clock and two endocrine pathways. Many studies have shown that the circadian clock is involved in the photoperiodic induction of diapause; however, how the clock affects the endocrine effector is not well understood. To evaluate this, we investigated the photoperiodic and temporal regulation of *Cyp15* and *jhamt* and the hemolymph JH titer. The function of *Cyp15* in photoperiodic ovarian development was also investigated. Furthermore, we examined the effect of RNAi targeted to *per* on ovarian development, expression of *Ilp1* and *Cyp15*, and hemolymph JH titer.

Materials and methods

Insects

Colonies of *R. pedestris* were established using individuals captured in Osaka, Japan (34.59°N, 135.51°E) in 2018–2021. Their progeny (G_1–G_3) were reared in a cylindrical cage (15 cm high and 15 cm diameter) in groups from the egg stage under diapause-inducing short-day (12 h light and 12 h dark; SD) conditions at 25 ± 1 °C. Within 24 h after adult emergence, the females were individually separated into small plastic cases (4 cm high and 10 cm diameter) and maintained under diapause-averting long-day (16 h light and 8 h dark; LD) conditions or were continuously kept under SD conditions. The insects were supplied with water containing 0.05% sodium ascorbate and 0.025% L-cysteine

(w/v), soybean grain, and red clover seeds (Kamano 1991). Day 0 was defined as the day of adult emergence.

Gene identification

We obtained the *Ilp1*, *Ilp2*, *jhamt*, and *Cyp15* sequences from the *R. pedestris* RNA-seq data (PRJDB7548 and PRJDB10569). The amino acid sequences of DILP2, DILP6, and JHAMT of *D. melanogaster*, Bombyxin A-1 and Bombyx IGF-like peptide (BIGFLP) from *Bombyx mori*, and Cyp15 A-1 of *Diploptera punctata* were used as queries in tBLASTn searches with the Bioedit program (Hall 1999). The accession numbers of these query sequences and sequences of *R. pedestris* are shown in Table 1.

ILPs can be divided into three classes based on their homology and C-peptide domain lengths estimated from the positions of two potential dibasic cleavable sites (Grönke and Partridge 2010; Mizoguchi and Okamoto 2013). To distinguish the classes, the amino acid sequences of ILP1 and ILP2 of *R. pedestris* were compared with those of the above-mentioned ILPs using ClustalW (Thompson et al. 1994). The signal peptide was estimated by signalP 5.0 (https://services.healthtech.dtu.dk/service.php?SignalP-5.0).

RT-qPCR

Reverse-transcription quantitative PCR (RT-qPCR) was performed to estimate the relative amount of target mRNA in the whole head with the prothorax (WH + PT), dorsocentral part of the brain (PI), brain and subesophageal ganglion without the PI (Br + SOG-PI), corpora cardiaca and CA with a part of the aorta (CC + CA), and fat body. Samples were collected at ZT 6–12. Total RNA was extracted using Trizol reagent (Thermo Fisher Scientific, Waltham, MA, USA) and treated with deoxyribonuclease (RT-grade) for Heat stop (NIPPON GENE, Toyama, Japan). cDNA was synthesized using a High-Capacity cDNA Reverse Transcription kit (Applied Biosystems, Foster City, CA, USA). Quantitative PCR was performed using a CFX connect™ Real-Time PCR Detection System (Bio-Rad, Hercules, CA, USA) according to the standard curve method with Go Taq qPCR Master Mix (Promega, Madison, WI, USA) and the primer sets shown in Table 2. *β-Tubulin* (*tub*) was used as a reference gene for normalization (Ikeno et al. 2011b).

Table 1 Accession numbers of amino acid and nucleotide sequences used in the present study

Amino acid/nucleotide	Species	Accession no
Amino acid		
BIGFLP	*Bombyx mori*	NP_001138796
BOMBYXIN A-1	*Bombyx mori*	XP_004934106
CYP15 A-1	*Diploptera punctata*	AAS13464.1
DILP2	*Drosophila melanogaster*	AAF50204
DILP6	*Drosophila melanogaster*	AAF45773
JHAMT	*Drosophila melanogaster*	AAF53533
Nucleotide		
CP-α	*Riptortus pedestris*	D87272
Cyp15	*Riptortus pedestris*	IADR01070114
Ilp1	*Riptortus pedestris*	ICRD01003192
Ilp2	*Riptortus pedestris*	ICRD01122962
jhamt	*Riptortus pedestris*	IADR01018524
per	*Riptortus pedestris*	AB379862
Vg-1	*Riptortus pedestris*	U97277

Immunohistochemistry

We prepared a rabbit polyclonal antibody against a nonapeptide (CGGSYNSPF), which is the C-terminal region of the ILP1 B-chain of *R. pedestris* (Cosmo Bio, Tokyo, Japan). The antibody was diluted by 1:1000 in 10% normal goat serum in phosphate-buffered saline (PBS) containing 0.1% Triton X-100 (PBSTx). A goat anti-rabbit IgG H&L conjugated with Alexa Fluor® 488 (Abcam, Cambridge, UK) was used as a secondary antibody at a 1:500 dilution in 10% normal goat serum in PBSTx.

The whole brains were dissected from adult females on day 13 in ice-cold PBS and fixed with 4% paraformaldehyde in PBSTx overnight. The antigen was retrieved in citrate buffer (pH 6.0) at 95 °C for 10 min and cooled at room temperature (18–25 °C) for 10 min. After washing in PBSTx and preincubation in 10% normal goat serum, the brain samples were incubated with primary antisera solution for 7 days at 4 °C. The brains were washed in PBSTx, preincubated in 10% normal goat serum, and incubated with the secondary antibody solution for 7 days at 4 °C. The brains were then washed with PBSTx and incubated with 4′,6-diamidino-2-phenylindole dihydrochloride (DAPI) at a final concentration of 100 ng/μL in PBS overnight. For fluorescence microscopy, the brains were dehydrated using an ethanol series (70%, 80%, 90%, 99%, and 100%) and cleared in methyl salicylate. The fluorescence of the samples was detected using confocal laser microscopy (DM6000CS, Leica Microsystems, Wetzlar, Germany) and analyzed with LAS X software (Leica Microsystems). The number of ILP1 immunoreactive (ILP1-ir) cells was estimated by counting the DAPI-stained nuclei in the ILP1-ir fluorescence images. Antibody specificity was confirmed in a preabsorption test, in which the primary antibody solution was preabsorbed with the synthesized nonapeptide at a final concentration of 10 μg/mL overnight at 4 °C.

Table 2 Nucleotide sequences of the primers used in this study

Gene	Primer name	Sequence (5'–3')
For dsRNA synthesis		
bla	blaF	TCG CCG CAT ACA CTA TTC TC
	blaR	TAC GAT ACG GGA GGG CTT AC
	blaT7F	GGA TCC TAA TAC GAC TCA CTA TAC GTC GCC GCA TAC ACT ATT CTC
	blaT7R	GGA TCC TAA TAC GAC TCA CTA TAC GTA CGA TAC GGG AGG GCT T
Cyp15	CYP15 F	TAC CGC TCT TGC CCT ACT CA
	CYP15 R	CGG CCA TTA GTG TCC AAA GA
	CYP15 T7F	TAA TAC GAC TCA CTA TAG GTA CCG CTC TTG CCC TAC TCA
	CYP15 T7R	TAA TAC GAC TCA CTA TAG GCG GCC ATT AGT GTC CAA AGA
Ilp1	ILP1F	GCC ATA GAA AAG GCA GAC CA
	ILP1R	TGC TCA GAC TCC TTT TGC AC
	ILP1T7F	TAA TAC GAC TCA CTA TAG GGC CAT AGA AAA GGC AGA CCA
	ILP1T7R	TAA TAC GAC TCA CTA TAG GTG CTC AGA CTC CTT TTG CAC
per	per F	GGG GAA GAT TTC TCC CGT AG
	per R	GAA CGT AGG GCA TTT GCT GT
	per T7F	TAA TAC GAC TCA CTA TAG GGG GGA AGA TTT CTC CCG TAG
	per T7R	TAA TAC GAC TCA CTA TAG GGA ACG TAG GGC ATT TGC TGT
For qPCR		
CP-α	CPα qF	TAG ACC TCT TGG TCG GAG TT
	CPα qR	CAG GAA CTC TCG TGG GTA TTT
Cyp15	CYP15 qF	CCC TTC CTT CGC TTT CTC TTA C
	CYP15 qR	GGA TCT CCT GTG ATC TTC AAC C
Ilp1	ILP1 qF	GAA CTT CTC CTC CTC TCT TTG G
	ILP1 qR	AAT CTG GGC AGA CCT CTT ATT C
Ilp2	ILP2 qF2	GGC TAC GCC ATA GGA AAT CAA
	ILP2 qR2	AGA ACT AGA GTT CGC CCT AAG A
jhamt	jhamt qF	GAT GCG GTC CAG GAG ATT T
	jhamt qR	GTC CAC TGC CGT CTT AGA TAT G
tub	tubul qpcr F	CTC AAC AAA TGT TCG ATG CTA AAA A
	tubul qpcr R	GCG ACC GTG CCT TGG A
Vg-1	Vg1 qF	TCA AGC CAG GCC AGA ATT AG
	Vg1 qR	CGT GTT GAT TGC TGT TTG AGA A

RNA interference

RNAi-mediated gene silencing was performed by double-stranded (ds) RNA injection. Total RNA was extracted from adult females as described above. cDNA was synthesized with oligo $(dT)_{12–18}$ primer and M-MLV reverse transcriptase (Thermo Fisher Scientific). The DNA template for dsRNA synthesis was amplified using the primers shown in Table 2 and Pwo Super Yield DNA polymerase (Roche, Basel, Switzerland). A T7 RiboMAX™ RNAi system (Promega) was used to synthesize the dsRNAs of *per*, *Cyp15*, and *Ilp1* according to the manufacturer's instruction. On day 0, the adults were anesthetized on ice, and their heads were injected with 1 µL of ds*Cyp15* (5 µg/µL), ds*per* (1 µg/µL), or ds*Ilp1* (1 µg/µL) RNA. The dsRNA of bacterial *β-lactamase* (*bla*), a control gene, was also synthesized and injected at the same concentration (1 or 5 µg/µL).

Fecundity and ovarian development

For the fecundity assay, adults were individually transferred to LD conditions on day 0. A single female and two males were placed in a single case on day 7, and the number of eggs deposited was recorded daily from days 8 to 20.

For ovarian development, adult females were dissected under a stereoscopic microscope and their ovaries were checked on day 13 or 20. The ovarian status was evaluated as described by Numata and Hidaka (1982): no oocytes as stage 0, one oocyte as stage I, two transparent oocytes as stage II, light-blue yolk deposition in the basal oocytes as stage III, light-blue yolk deposition in two oocytes as stage IV,

and post-ovulation as stage V. Females in stages 0–II were considered to be in diapause and those in stages III–V were considered as non-diapause (Numata and Hidaka 1982).

Hemolymph JH quantification

To collect the hemolymph, a decapitated adult female was placed head-down in a perforated 0.5 mL tube inserted in a 1.5 mL silicon-coated tube. The tube was centrifuged at 100 × *g* for 5 min at 4 °C, and the collected hemolymph was stored at -80 °C until use.

Hemolymph sample preparation and ultra-performance liquid chromatography–tandem mass spectrometry (UPLC–MS/MS) analysis were performed as described by Ando et al. (2020) and Lee et al. (2019). Briefly, 16–20 µL of hemolymph from 4 to 18 individuals was added to 200 pg of synthetic JH III (internal control; Sigma-Aldrich, St. Louis, MO, USA). The sample was mixed with 500 µL of methanol and incubated for 5 min on ice. After adding 500 µL of 2% NaCl solution (w/v), the sample was extracted with 200 µL of hexane, and the supernatant was transferred to another tube after centrifugation at 3000 × *g* for 5 s. This process was repeated 3 times. The pooled extract was dried in a centrifugal evaporator (CVE-2200, EYELA, Tokyo, Japan). The sample was suspended in 20 µL of methanol and transferred to a dedicated tube (Autosampler vial #186000385C, Waters, Milford, MA, USA). This process was repeated 2 times.

The UPLC–MS/MS (ACQUITY UPLC H-Class, Xevo TQ-S micro, Waters) and a C18 column (ACQUITY UPLC BEH C18 Column, 2.1 × 100 mm, 1.7 µm particle size, Waters) were used to detect $JHSB_3$ and JH III with MassLynks software (Waters). The solvent for the C18 column was water: methanol = 2:8, and the flow rate was 0.2 mL/min. MS/MS analysis revealed the fragment ions of $JHSB_3$ and JH III at $m/z = 283.2 > 233.2$ and $m/z = 267.3 > 43.0$, respectively (Ando et al. 2020). The hemolymph $JHSB_3$ concentration was corrected according to the peak area of the control JH III.

Statistical analysis

The statistical analysis was conducted in R Studio Version 2022.2.0.443 and R version 4.1.2.

Results

ILP classes

tBlastn searches detected two *Ilp* sequences, *Ilp1* and *Ilp2*. Insect ILPs can be divided into 3 classes, i.e., ILP (sensu stricto), IGFLP, and DILP7-like (Grönke and Partridge 2010). To determine the classes of *Ilp1* and *Ilp2*, their amino acid sequences and domain structures were compared with those of ILPs from other insect species (Fig. 1). The *R. pedestris* ILP1 amino acid sequence contained a long C-peptide, which is characteristic of members of the ILP (sensu stricto) class including DILP2 and Bombyxin A-1 (Fig. 1, upper panel). The positions of cysteine residues and dibasic cleavable sites were well conserved among species. The *R. pedestris* ILP2 amino acid sequence contained a short C-peptide, which is characteristic of members of the IGFLP class including DILP6 and BIGFLP (Fig. 1, lower panel). The positions of the cysteine residues were also conserved.

Expression of *Ilp1* and *Ilp2*

We investigated the photoperiodic and temporal changes in *Ilp* expression (Fig. 2a). The relative amount of *Ilp1* mRNA gradually increased from days 5 to 13 under LD conditions (4.1-fold increase compared to the median), whereas no temporal change was detected under SD conditions. The amount of *Ilp1* mRNA was significantly higher in LD than in SD on day 13 (3.1-fold increase compared to the median; Student's *t* test, $P < 0.05$), but not on other days (Student's *t* test, $P > 0.05$). The relative amounts of *Ilp2* mRNA did not change temporally and photoperiodically (day 5; Welch's *t* test, days 9 and 13; Student's *t* test, $P > 0.05$). RT-qPCR analysis revealed that *Ilp1* was highly expressed in the PI (Fig. 2b).

Immunohistochemical staining verified specific ILP1 expression in the PI; the antibody against *R. pedestris* ILP1 detected ILP1-ir cells in the dorsocentral part of the brain (Fig. 3a–c). Absorption control experiment for the ILP1 antibody revealed autofluorescence only in the retina, confirming the specificity of the ILP1 antibody (data not shown). The most frequent number of ILP1-ir cells was six in each hemisphere and was identical between photoperiodic conditions (Fig. 3d).

Effects of *Ilp1* RNAi on egg number and yolk protein expression

Injection of ds*Ilp1* effectively downregulated *Ilp1* expression (91.3% reduction compared to the median; Welch's *t* test, $P < 0.05$) (Fig. 4a). Control females laid an average of 2.64–5.55 eggs every day. Females injected with ds*Ilp1* also laid eggs but their daily number was 1.77–4.08, which was significantly smaller than the number of control females (two-way ANOVA, $P < 0.05$) (Fig. 4b). *Ilp1* RNAi did not affect the expression of the yolk proteins *Vg-1* and *CP-α* in the fat body (Fig. 4c; Student's *t* test, $P > 0.05$), suggesting that the low fecundity of *Ilp1* RNAi females was not caused by downregulation of yolk proteins.

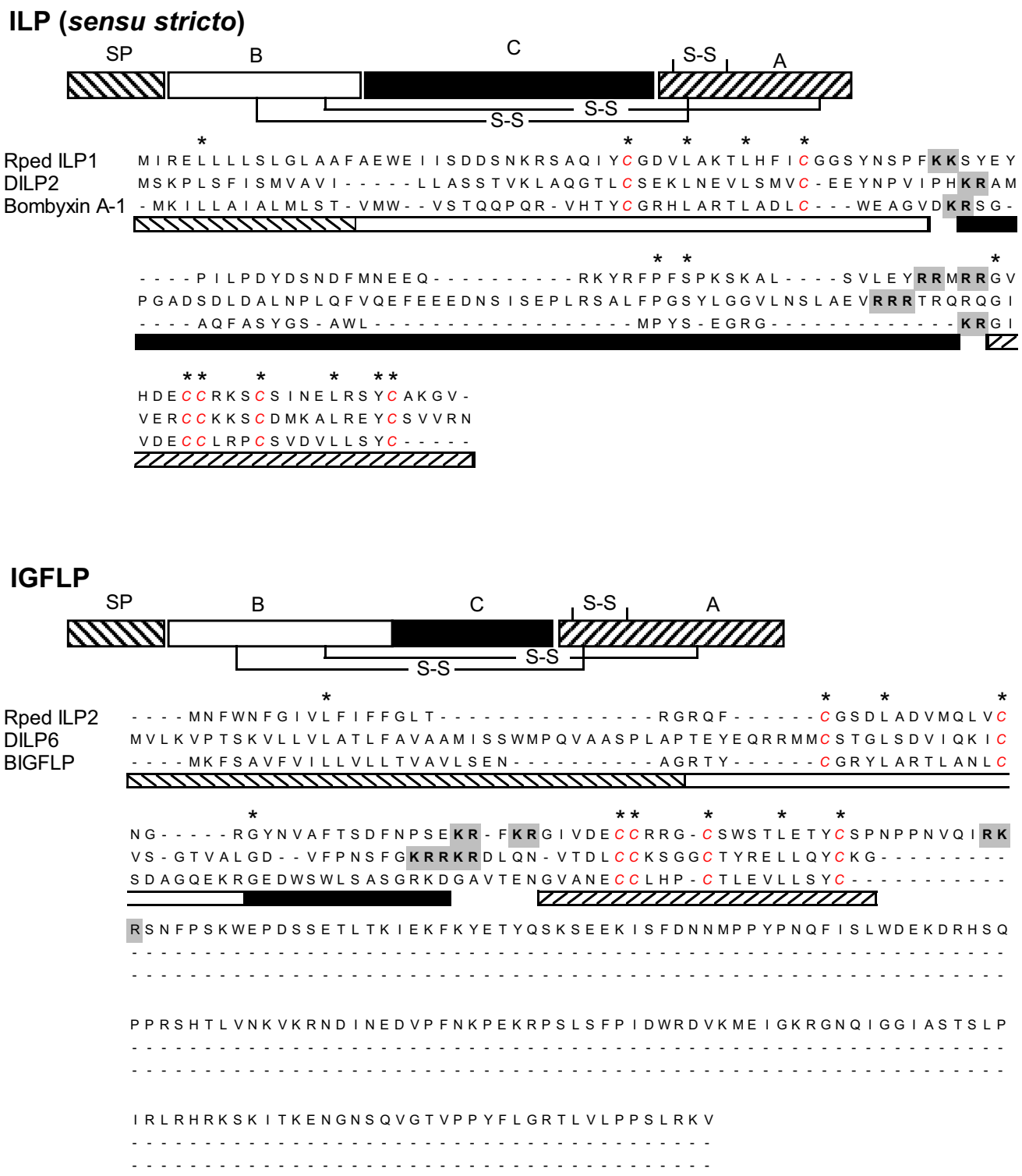

Fig. 1 Structures and amino acid sequences of ILPs (sensu stricto) (upper panel) and IGFLPs (lower panel). Rped ILP1 and Rped ILP2 are from *Riptortus pedestris*, DILP2 and DILP6 are from *Drosophila melanogaster*, and Bombyxin A-1 and BIGFLP are from *Bombyx mori*. Predicted domains of the A- and B-chains, C-peptide, and signal peptide (SP) are shown in boxes. "S–S" indicates the disulfide bond. Asterisks indicate conserved amino acid residues. Potential cleavage sites estimated by dibasic amino acids are shown with shaded letters. Italicized "*C*" indicates conserved cysteine residue. For accession numbers, see Table 1

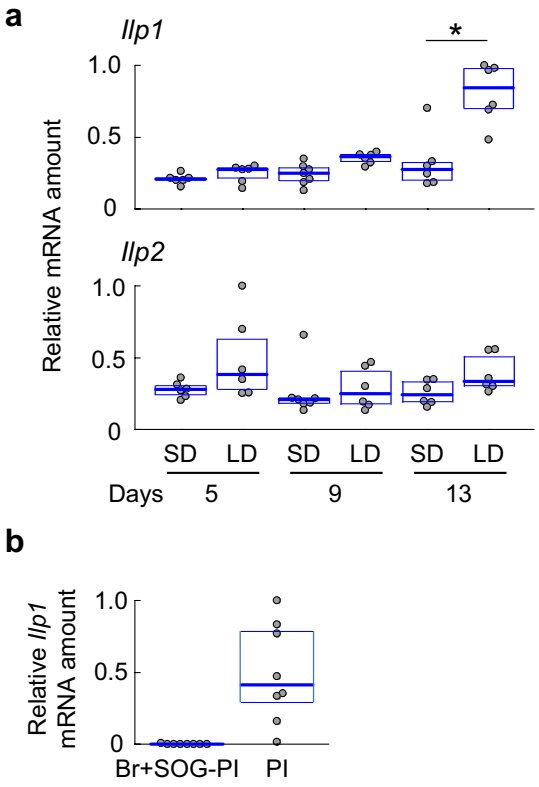

Fig. 2 Expression profiles of *Ilp1* and *Ilp2*. **a** Amounts of *Ilp1* and *Ilp2* mRNAs in the whole head with the prothorax (WH + PT) of virgin adult females on days 5, 9, and 13 under short-day (SD) and long-day (LD) conditions. $n = 6–7$. *, The Student's t test ($P < 0.05$). **b** *Ilp1* mRNA amounts in the brain and subesophageal ganglion without the pars intercerebralis (Br + SOG-PI) and pars intercerebralis (PI) on day 13 under LD conditions. $n = 8$. Each plot indicates a sample from a single individual. The highest value was set at 1.0. The middle line in the box indicates the median, and the upper and lower lines of the box indicate the quartile

Hemolymph JHSB3 concentration and Cyp15 and jhamt expression

The photoperiodic and temporal profiles of $JHSB_3$ concentrations in the hemolymph are shown in Fig. 5a. The $JHSB_3$ concentration increased under LD conditions (two-way ANOVA, $P < 0.05$). The $JHSB_3$ concentration increased from days 9–13 (3.6-fold increase compared to the average), but decreased on day 20 under LD conditions. By contrast, the $JHSB_3$ concentration remained low under SD conditions, irrespective of the days after adult emergence (Fig. 5a).

We further investigated temporal and photoperiodic regulation of *Cyp15* and *jhamt*. Under LD conditions, *Cyp15* expression increased from days 5 to 9 and remained high on day 13. The amounts were consistently higher under LD than SD on all dates (3.3–6.8-fold increase compared to the median; Welch's t test, $P < 0.05$) (Fig. 5b). The relative amounts of *jhamt* mRNA gradually increased from days 5–13, with no or little photoperiodic change (Student's t test, $P > 0.05$) (Fig. 5b). *Cyp15* was highly expressed in the CC–CA complex (Fig. 5c).

Effects of *Cyp15* RNAi on ovarian development

Cyp15 mRNA amounts were significantly lower in females injected with ds*Cyp15* than in control (ds*bla*-injected) females on day 13 under LD conditions (74% reduction compared to the median) (Fig. 6a, Student's t test, $P < 0.05$). Ovarian development was affected by *Cyp15* RNAi; the proportion of females that had ovulated mature eggs (stage V) was 88.0% in the ds*bla*-injected group, whereas that in the ds*Cyp15* group was only 42.4% (Fig. 6b), which was a significant difference (Mann–Whitney U test; $P < 0.05$).

Effects of *per* RNAi on *Ilp1* and *Cyp15* expression

We focused on the role of the circadian clock in endocrine regulation. Injection of ds*per* weakly but significantly reduced *per* mRNA amounts (24% reduction compared to the median) (Fig. 7a, Welch's t test, $P < 0.05$). RNAi targeted to *per* increased the number of vitellogenic females (Fig. 7b, Fisher's exact test, $P < 0.05$). RNAi targeted to *per* also significantly induced *Ilp1* and *Cyp15* expression on day 20 under SD conditions (1.9- and 4.8-fold increment compared to the median, respectively) (Fig. 7c; Student's t test, $P < 0.05$), suggesting that these genes reside downstream of the circadian clock. Upregulation of *Cyp15* via *per* RNAi was reflected as an increment in hemolymph $JHSB_3$ concentrations (Fig. 7d, Welch's t test, $P = 0.089$).

Discussion

Both ILP (sensu stricto) and IGFLP regulate systemic growth, but their expression sites and regulatory elements differ. ILPs are mainly expressed in the PI in the brain and regulated by sugars in the hemolymph, peptides from the peripheral tissues, and neurotransmitters in the brain. By contrast, IGFLPs are mainly expressed in the fat body and regulated by nutrients such as amino acids, lipids, and carbohydrates in the hemolymph (Nässel and Broeck 2015; Okamoto and Yamanaka 2015). We found that in *R. pedestris*, *Ilp1*, which belongs to the ILP (sensu stricto) class, was downregulated under SD conditions, whereas *Ilp2*, which belongs to the IGFLP class, was not regulated in a photoperiodic manner. Photoperiodic regulation of ILPs was also reported in other insect species. In *C. pipiens*, genes encoding ILP-1 and ILP-5 are downregulated in diapausing females, but a gene encoding ILP-2 is not downregulated (Sim and Denlinger 2009). In *A. pisum*, *Ilp1* and *Ilp4* are downregulated under SD conditions, which are sexual

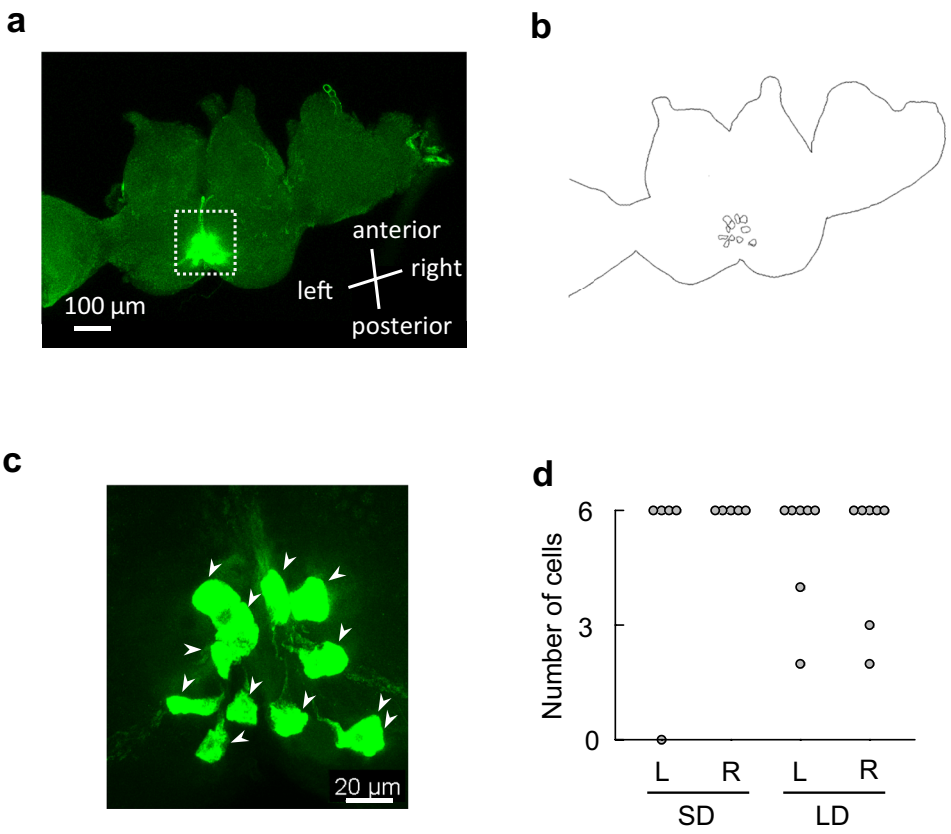

Fig. 3 Immunofluorescence of ILP1 in the whole brain of adult female *Riptortus pedestris*. **a** ILP1 immunoreactive(ir)-cells in dorsal view of the whole brain. **b** Schematic drawing of **a**. **c** Enlarged photo inside of the dashed line in **a**. Twelve ILP1-ir cells were detected (arrowheads). **d** Number of ILP1-ir cells detected in the left (L) and right (R) brain hemispheres under short-day (SD) and long-day (LD) conditions. $n = 5–7$

morphs producing conditions. (Barberà et al 2019; Cuti et al. 2021). We verified that ILP1 is specifically expressed in the PI of *R. pedestris*. The single-cell PCR also supported ILP1 expression in the PI of this species (Hasebe and Shiga 2021).

In *C. pipiens*, RNAi targeted to the genes encoding insulin-like receptor and ILP-1 suppressed photoperiodic ovarian development, whereas JH III and JH analogs rescued this suppression (Sim and Denlinger 2008, 2009). In *D. melanogaster*, in which dormancy is regulated by JH (Kurogi et al. 2021), ovarian development was found to be more retarded in *Ilp2-3*- and *Ilp5*-deficient mutants than in control flies (Kubrak et al. 2014). An extensive genetic dissection of the insulin signaling pathway verified that ILP2 and ILP5 are key antagonists of ovarian arrest (Schiesari et al. 2016). Ojima et al. (2018) further revealed in *D. melanogaster* that insulin signaling, initiated in insulin-producing cells in the brain, regulates the insulin cascade in the CA to induce yolk accumulation in the egg by stimulating JH biosynthesis. Thus, in these species, ILP resides upstream of the JH biosynthesis pathway and controls the JH biosynthetic process to regulate the photoperiodic response (Kurogi et al. 2021; Sim and Denlinger 2013a); however, this is not the case in *R. pedestris*. The present study revealed that *Ilp1* regulated fecundity, but this effect was not caused by suppression of yolk protein expression. Hasebe and Shiga (2021) also demonstrated in *R. pedestris* that *Ilp1* is important in promoting oviposition but plays no or little role in ovarian development. Previous studies revealed that yolk protein expression and ovarian development are regulated by JH in this species (Hirai et al. 1998; Miura et al. 1998). Furthermore, surgical removal of the PI, which contains insulin-producing cells, did not affect photoperiodic ovarian development but affected fecundity in *R. pedestris* (Shimokawa et al. 2008, 2014). Thus, in *R. pedestris*, ILP1 does not reside upstream of JH signaling. The ILP and JH signaling pathways independently regulate different photoperiodic events.

Next, we focused on photoperiodic regulation of *jhamt* and *Cyp15* in the JH biosynthesis pathway. Their important roles in the JH biosynthetic process have been verified in various insect species (Daimon et al. 2012; Helvig et al. 2004; Li et al. 2013; Marchal et al. 2011; Minakuchi et al. 2008; Niwa et al. 2008; Nouzova et al. 2021; Shinoda and Itoyama 2003). In the present study, photoperiodic regulation of *jhamt* was undetectable, in contrast to that of *Cyp15*. *Cyp15* expression was suppressed under SD conditions compared to that under LD conditions, in which *Cyp15* was expressed in the CC–CA complex. In addition, *Cyp15* suppression was associated with a low hemolymph $JHSB_3$ concentration under SD conditions. We also found that *Cyp15* RNAi suppressed ovarian development. These results suggest that *Cyp15* is the photoperiodic regulator in the JH biosynthesis cascade in the CA of *R. pedestris*. The

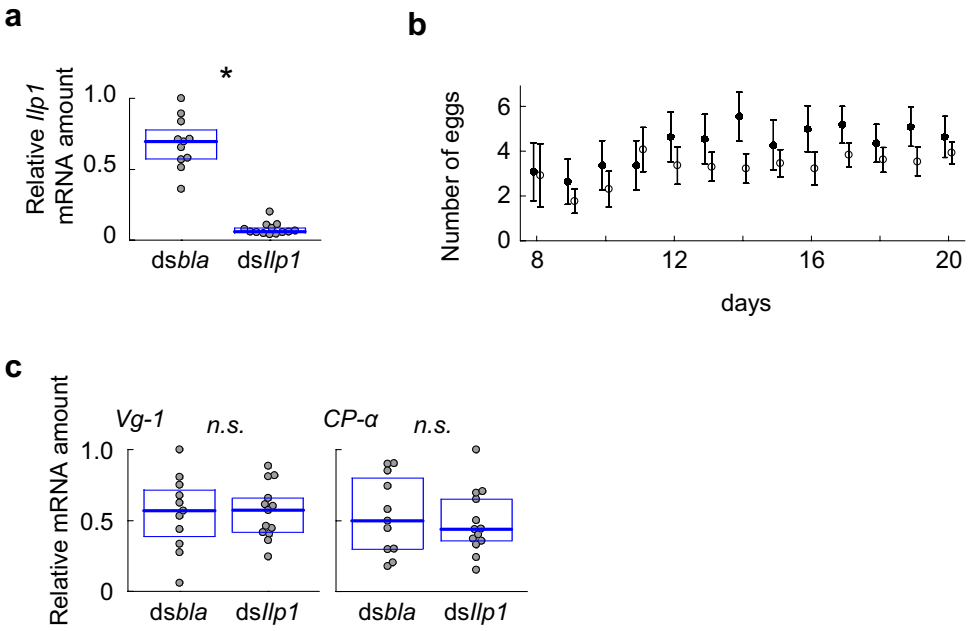

Fig. 4 Effects of *Ilp1* dsRNA injection on *Ilp1* mRNA amounts (**a**) number of eggs deposited (**b**), and *Vg-1* and *CP-α* mRNA amounts (**c**) in adult females of *Riptortus pedestris* under long-day conditions. **a** *Ilp1* mRNA amounts in the whole head with the prothorax (WH + PT) on day 20 are shown. Each plot indicates a sample from a single individual. An asterisk indicates a significant difference (Welch's *t* test, $P < 0.05$). $n = 11$–13. **b** Number of eggs deposited each day. Females were individually reared with two males, and the number of eggs was counted every day. Closed and open circles indicate the mean egg numbers in ds*bla*- ($n = 11$) and ds*Ilp1*-injected ($n = 13$) females, respectively. The error bars indicate the standard errors. Two-way ANOVA revealed a significant difference between ds*bla*- and ds*Ilp1*-injected females ($P = 0.0075$) but not among days ($P = 0.427$). No interaction was detected ($P = 0.988$). **c** *Vg-1* and *CP-α* mRNA amounts in the fat body on day 20. Each plot indicates a sample from a single individual. $n = 11$–13. *n.s.,* no significant difference (Student's *t* test, $P > 0.05$). The middle line in the box indicates the median, and the upper and lower lines of the box indicate the quartile in **a** and **c**

roles of *jhamt* and *Cyp15* in photoperiodic diapause have also been examined in several insect species. For example, both *jhamt* and *Cyp15* are downregulated in diapause-destined females of the cabbage beetle *Colaphellus bowringi* (Tian et al. 2021). Similar results were obtained in diapausing *Danaus plexippus* (Zhan et al. 2011). In contrast to in *R. pedestris*, RNAi targeted to *Cyp15* did not decrease ovarian development in *C. bowringi*, whereas RNAi targeted to *jhamt* did (Tian et al. 2021). The function of *Cyp15* in the photoperiodic signaling pathway may be species-specific.

Although RNAi of circadian clock genes verified the involvement of the circadian clock in photoperiodism in various species (Goto 2022), it has been veiled how the clock regulates endocrine signaling pathways. The present study revealed that RNAi targeted to *per* induced *Ilp1* and *Cyp15* expression, boosted hemolymph JH concentrations, and finally induced ovarian development. These results indicate that the circadian clock governs the photoperiodic response by altering the expression of key elements in two endocrine pathways. In the brain of *R. pedestris*, two PER-ir cells are located in an anterior medial region of the medulla, which is close to the accessory medulla, and named as "lateral neuron lateral (LNl)" cells (Koide et al. 2021). Microsurgical removal of the region containing these PER-ir cells disrupted photoperiodic ovarian development, suggesting that LNl cells act as clock cells in the photoperiodic response (Ikeno et al. 2014; Koide et al. 2021). In *R. pedestris*, photoperiodic ovarian development is not controlled by a neuropeptide pigment-dispersing factor, but possibly by the neurotransmitter glutamate (Des Marteaux et al. 2022; Ikeno et al. 2014). The importance of glutamate as a circadian output element was previously verified in *D. melanogaster* (Collins et al. 2012; Guo et al. 2016). The circadian clock that includes *per* may use glutamate to control *Cyp15* expression in the CA and regulates photoperiodic ovarian development through the hemolymph JH concentration, which requires further investigation.

Furthermore, studies are needed for neuroanatomical dissection and functional verification of the LNl cells and pars lateralis neurons, which innervate the CA and suppress CA activity (Shimokawa et al. 2008). It is also important to verify the CA regulatory factors in the pars lateralis neurons. Possible candidates would for these regulatory factors include allatotropin (Kang et al. 2014), allatostatin (Matsumoto et al. 2017; Tamai et al. 2019), myosuppressin (Miki et al. 2020), ecdysteroids, and ecdysis-triggering hormone

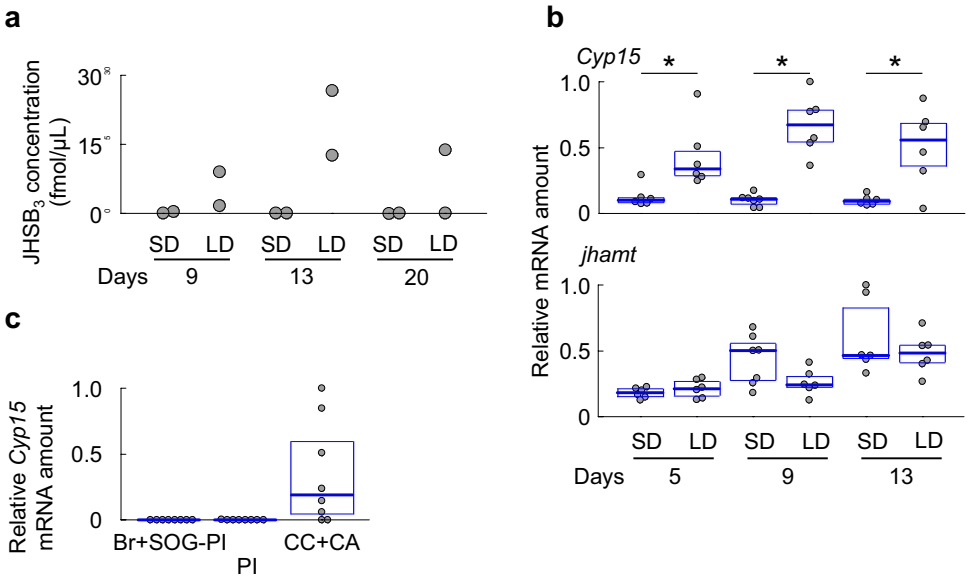

Fig. 5 Hemolymph $JHSB_3$ concentration and *Cyp15* and *jhamt* expression profiles. **a** Hemolymph $JHSB_3$ concentrations on days 9, 13, and 20 under short-day (SD) and long-day (LD) conditions. Each plot was obtained from 20 μL of hemolymph. $n=2$. Two-way ANOVA revealed a significant difference between SD and LD ($P<0.05$). **b** Amounts of *Cyp15* and *jhamt* mRNAs in the whole head with the prothorax (WH+PT) of virgin adult females on days 5, 9, and 13 under short-day (SD) and long-day (LD) conditions. $n=6$–7. A significant difference between SD and LD was detected in *Cyp15* (Welch's *t* test, $P<0.05$), but not in *jhamt* (Student's *t* test, $P>0.05$). **c** Amounts of *Cyp15* mRNA in the brain and subesophageal ganglion without the pars intercerebralis (Br+SOG-PI), pars intercerebralis (PI), and corpus allatum with the corpora cardiaca (CC+CA). $n=8$. Each plot indicates a sample from a single individual in **b** and **c**. The highest value was set at 1.0, and the middle line in the box indicates the median and the upper and lower lines indicate the quartile in **b** and **c**

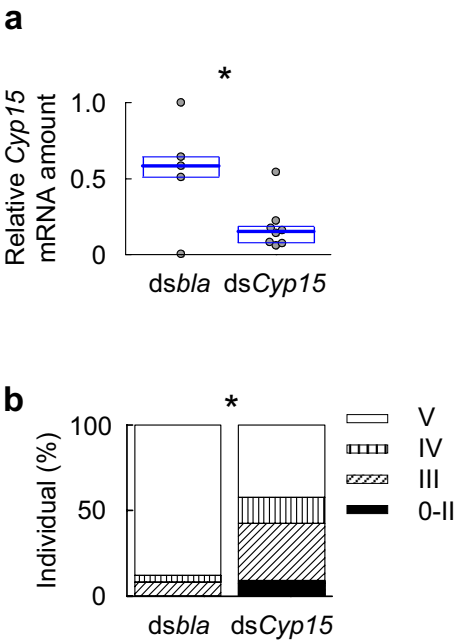

Fig. 6 Effects of *Cyp15* dsRNA injection on *Cyp15* mRNA amounts (**a**) and ovarian development (**b**) in virgin adult females of *Riptortus pedestris* under long-day conditions on day 13. **a** *Cyp15* mRNA amounts in the whole head with the prothorax (WH+PT). Each plot represents a sample from a single individual. $n=5$–8. The middle line in the box indicates the median, and the upper and lower lines indicate the quartile. An asterisk indicates a significant difference (Student's *t* test, $P<0.05$). **b** Ovarian stages. $n=25$–33. The asterisk indicates a significant difference (Mann–Whitney *U* test, $P<0.001$)

(Guo et al. 2021). How the circadian clock regulates ILP1 expression remains unknown in *R. pedestris*, although other insect species provide some clues. In the kissing bug *Rhodnius prolixus*, both the production and axonal transport of ILPs show a daily rhythm and intimate associations with the ILP and pigment-dispersing factor axons in both the central brain and retrocerebral complex (Steel and Vafopoulou 2006; Vafopoulou and Steel 2012, 2014). The results suggest a neural connection. In *D. melanogaster*, a subset of circadian clock neurons, posterior dorsal neuron 1, makes synaptic contact with insulin-producing cells in the PI (Barber et al. 2016) and regulates circadian oogenesis with a neuropeptide allatostatin C (Zhang et al. 2021). In addition, two circadian output neuropeptides, pigment-dispersing factor and short neuropeptide F, synergistically inhibit reproductive dormancy, likely by modulating the activity of insulin-producing cells (Nagy et al. 2019). Studies are needed to investigate the neuroanatomy of LNl cells and PI cells expressing ILPs and the roles of these neuropeptides in fecundity in *R. pedestris*.

Here, we summarize the molecular cascade regulating photoperiodic adult diapause in *R. pedestris*, which is partially different from that in *C. pipiens* (Fig. 8). In *C. pipiens*, ILP-1 regulates reproduction under long days through two pathways; it resides upstream of the CA and regulates

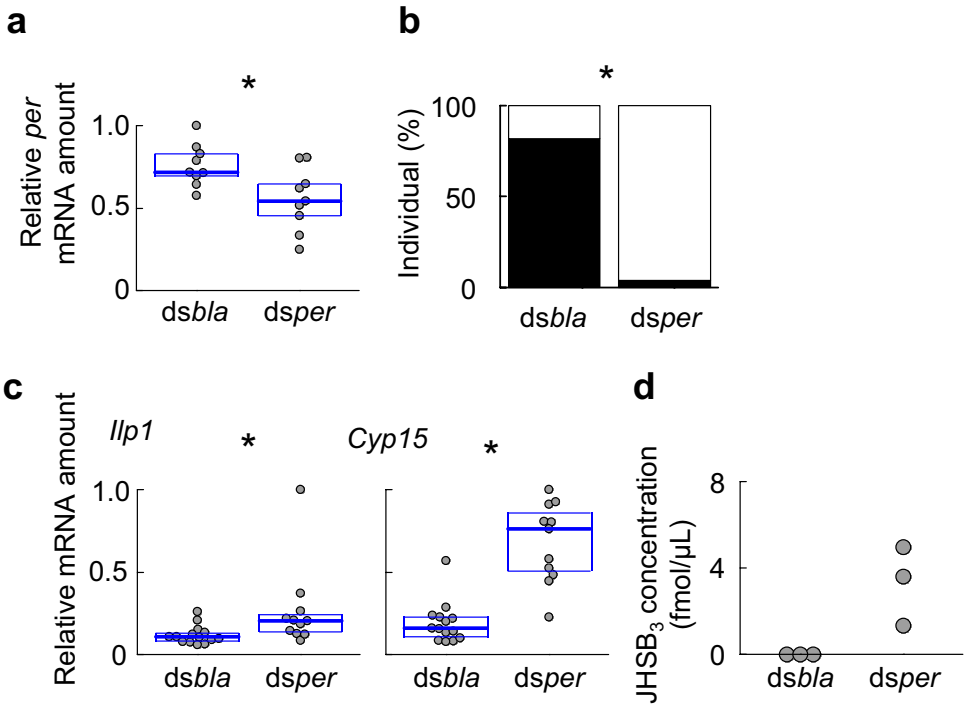

Fig. 7 Effect of *per* dsRNA injection on *per* mRNA amount (**a**), ovarian development (**b**), *Ilp1* and *Cyp15* mRNA amounts (**c**), and hemolymph $JHSB_3$ concentration (**d**) in virgin adult females of *Riptortus pedestris* under short-day conditions. **a** *per* mRNA in the brain with the subesophageal ganglion on day 3. Each point represents a sample from a single individual. $n=9$. **b** Ovarian development on day 13. The closed and open columns indicate non-vitellogenic (stages 0–II) and vitellogenic (stages III–V) individuals, respectively. **c** *Cyp15* and *Ilp1* mRNAs in the head with the prothorax (WH+PT) on day 13. Each point represents a sample from a single individual. $n=11$–14. **d** Hemolymph $JHSB_3$ concentration on day 13. Each plot represents $JHSB_3$ concentration from 16 μL of the hemolymph. $n=3$. The middle line in the box indicates the median, and the upper and lower lines indicate the quartile in **a** and **c**. A significant difference (indicated by an asterisk) between ds*bla* and ds*per* injection was detected in **a** (Welch's *t* test, $P<0.05$), **b** (Fisher's exact test, $P<0.05$), and **c** (Student's *t* test, $P<0.05$), but not in **d** (Welch's *t* test, $P=0.089$)

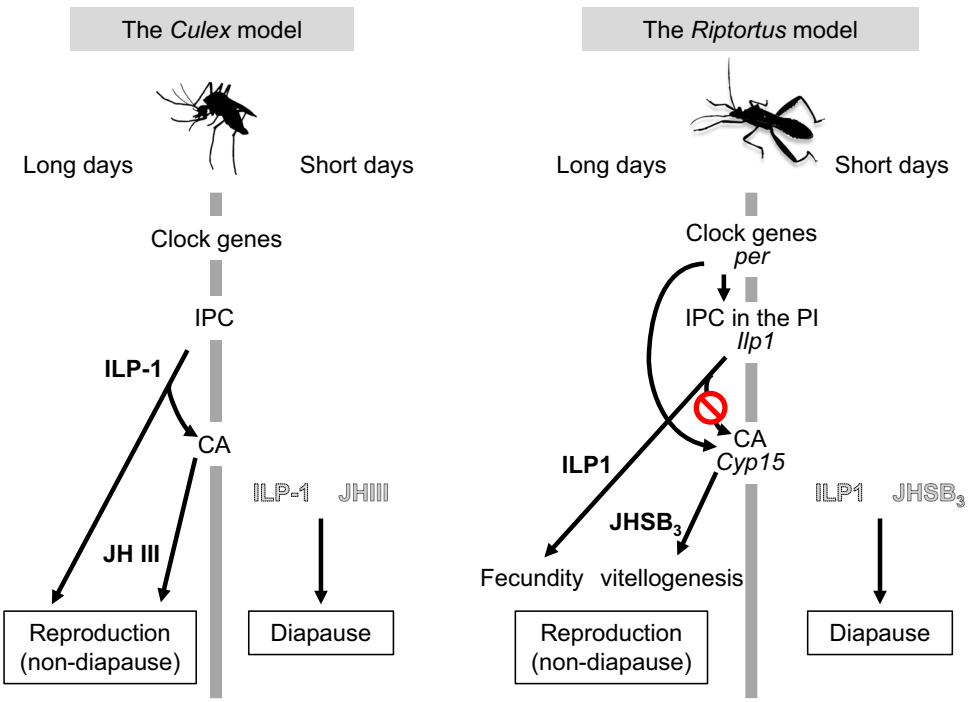

Fig. 8 Regulatory pathways of photoperiodic responses in *Culex pipiens* (left panel) and *Riptortus pedestris* (right panel). ILPs regulate the JH pathway in *C. pipiens* but not in *R. pedestris,* in which ILP and JH independently regulate reproduction. *CA* corpus allatum, *Cyp15* cytochrome P450 15 gene, *ILP* insulin-like peptide, *IPC* ILP-producing cell, *per*, *period* gene, *PI* pars intercerebralis. For further explanation, see the main text

JH production and also regulates the physiological status of the output module directly (Readio et al. 1999; Sim and Denlinger 2008, 2009, 2013a, b). The circadian clock genes govern the photoperiodic response, but it is still unknown how they regulate downstream endocrine elements (Chang and Meuti 2020; Meuti et al. 2015; Peffers and Meuti 2022). In *R. pedestris*, ILP1 regulates fecundity and sugar homeostasis (Hasebe and Shiga, 2021; the present study), and *Cyp15* regulates vitellogenesis and ovarian development through $JHSB_3$ biosynthesis (Ando et al. 2020; the present study). ILP1 does not regulate JH-dependent vitellogenesis and ovarian development (Shimokawa et al. 2008; Hasebe and Shiga 2021; the present study). The circadian clock including *per* governs the photoperiodic response (Ikeno et al. 2010) and this clock regulates the expression of *Ilp1* in the PI and *Cyp15* in the CA (the present study). Our results provide insight into the molecular linkage between the circadian clock and endocrine effectors.

Acknowledgements We appreciate Dr. Tetsuro Shinada (Osaka Metropolitan University) for supplying the synthesized $JHSB_3$. We also appreciate Dr. Akira Mizoguchi (Aichi Gakuin University) for his advice on the target sequence of the anti-ILP1 antibody. We would like to thank Dr. Taro Fuchikawa (Osaka Metropolitan University) for his advice on immunostaining.

Author contributions Authors contributed to the study conception and design. Material preparation, data collection, analysis, and first draft of the manuscript were performed by Genyu Mano. Authors commented on previous versions of the manuscript and approved the final manuscript.

Funding This work was supported by JST SPRING (JPMJSP2139) to GM and Grant-in-Aid for Scientific Research B (22H02361) to SGG. The authors have no relevant financial or non-financial interests to disclose.

Declarations

Conflict of interest The authors declare that they have no conflict of interest.

References

Ando Y, Matsumoto K, Misaki K et al (2020) Juvenile hormone III skipped bisepoxide, not its stereoisomers, as a juvenile hormone of the bean bug *Riptortus pedestris*. Gen Comp Endocrinol 289:113394. https://doi.org/10.1016/j.ygcen.2020.113394

Barber AF, Erion R, Holmes TC, Sehgal A (2016) Circadian and feeding cues integrate to drive rhythms of physiology in *Drosophila* insulin-producing cells. Genes Dev 30:2596–2606. https://doi.org/10.1101/gad.288258.116

Barberà M, Cañas-Cañas R, Martínez-Torres D (2019) Insulin-like peptides involved in photoperiodism in the aphid *Acyrthosiphon pisum*. Insect Biochem Mol Biol 112:103185. https://doi.org/10.1016/j.ibmb.2019.103185

Broughton SJ, Piper MDW, Ikeya T et al (2005) Longer lifespan, altered metabolism, and stress resistance in *Drosophila* from ablation of cells making insulin-like ligands. Proc Natl Acad Sci USA 102:3105–3110. https://doi.org/10.1073/pnas.0405775102

Chang V, Meuti ME (2020) Circadian transcription factors differentially regulate features of the adult overwintering diapause in the Northern house mosquito *Culex Pipiens*. Insect Biochem Mol Biol 121:103365. https://doi.org/10.1016/j.ibmb.2020.103365

Collins B, Kane EA, Reeves DC, Akabas MH, Blau J (2012) Balance of activity between LN_Vs and glutamatergic dorsal clock neurons promotes robust circadian rhythms in *Drosophila*. Neuron 74:706–718. https://doi.org/10.1016/j.neuron.2012.02.034

Cuti P, Barberà M, Veenstra JA, Martínez-Torres D (2021) Progress in the characterization of insulin-like peptides in aphids: Immunohistochemical mapping of ILP4. Insect Biochem Mol Biol 136:103623. https://doi.org/10.1016/j.ibmb.2021.103623

Daimon T, Kozaki T, Niwa R et al (2012) Precocious metamorphosis in the juvenile hormone–deficient mutant of the silkworm, *Bombyx mori*. Plos Genet 8:e1002486. https://doi.org/10.1371/journal.pgen.1002486

Danks HV (1987) Insect Dormancy: An Ecological Perspective. Biological Survey of Canada, Ottawa

de Kort CAD, Bergot BJ, Schooley DA (1982) The nature and titre of juvenile hormone in the Colorado potato beetle, *Leptinotarsa decemlineata*. J Insect Physiol 28:471–474. https://doi.org/10.1016/0022-1910(82)90077-4

Denlinger DL (2022) Insect Diapause. Cambridge University Press, Cambridge

Des Marteaux L, Xi J, Mano G, Goto SG (2022) Circadian clock outputs regulating insect photoperiodism: A potential role for glutamate transporter. Biochem Biophys Res Commun 589:100–106. https://doi.org/10.1016/j.bbrc.2021.12.014

Goltzené F, Holder F, Charlet M et al (1992) Immunocytochemical localization of *Bombyx*-PTTH-like molecules in neurosecretory cells of the brain of the migratory locust, *Locusta migratoria*. Cell Tissue Res 269:133–140. https://doi.org/10.1007/BF00384733

Goodman WG, Cusson M (2012) The Juvenile Hormones. In: Gilbert LI (ed) Insect Endocrinology. Academic Press, Oxford, pp 310–365

Goto SG (2022) Photoperiodic time measurement, photoreception, and circadian clocks in insect photoperiodism. Appl Entomol Zool 57:193–212. https://doi.org/10.1007/s13355-022-00785-7

Goto SG, Nagata M (2022) The circadian clock gene (*Clock*) regulates photoperiodic time measurement and its downstream process determining maternal induction of embryonic diapause in a cricket. Eur J Entomol 119:12–22. https://doi.org/10.14411/EJE.2022.002

Grönke S, Partridge L (2010) The Functions of Insulin-like Peptides in Insects. In: Clemmons D, Robinson I, Christen Y (Eds) IGFs:Local Repair and Survival Factors Throughout Life Span. Research and Perspectives in Endocrine Interactions. Springer, Heidelberg, pp 105–124. https://doi.org/10.1007/978-3-642-04302-4_9

Guo S-S, Zhang M, Liu T-X (2016) Insulin-related peptide 5 is involved in regulating embryo development and biochemical composition in pea aphid with wing polyphenism. Front Physiol 9:7–31. https://doi.org/10.3389/fphys.2016.00031

Guo S, Tian Z, Wu Q-W et al (2021) Steroid hormone ecdysone deficiency stimulates preparation for photoperiodic reproductive diapause. PLoS Genet 17:e1009352. https://doi.org/10.1371/journal.pgen.1009352

Hall TA (1999) BIOEDIT: a user-friendly biological sequence alignment editor and analysis program for Windows 95/98/ NT. Nucl Acids Symp Ser 41:95–98

Hasebe M, Shiga S (2021) Oviposition-promoting pars intercerebralis neurons show *period*-dependent photoperiodic changes in their firing activity in the bean bug. Proc Natl Acad Sci USA 118:e2018823118. https://doi.org/10.1073/pnas.2018823118

Hejníková M, Nouzova M, Ramirez CE et al (2022) Sexual dimorphism of diapause regulation in the hemipteran bug *Pyrrhocoris apterus*. Insect Biochem Mol Biol 142:103721. https://doi.org/10.1016/j.ibmb.2022.103721

Helvig C, Koener JF, Unnithan GC, Feyereisen R (2004) CYP15A1, the cytochrome P450 that catalyzes epoxidation of methyl farnesoate to juvenile hormone III in cockroach corpora allata. Proc Natl Acad Sci USA 101:4024–4029. https://doi.org/10.1073/pnas.0306980101

Hirai M, Yuda M, Shinoda T, Chinzei Y (1998) Identification and cDNA cloning of novel juvenile hormone responsive genes from fat body of the bean bug, *Riptortus clavatus* by mRNA differential display. Insect Biochem Mol Biol 28:181–189. https://doi.org/10.1016/S0965-1748(97)00116-1

Hodková M (1976) Nervous inhibition of corpora allata by photoperiod in *Pyrrhocoris apterus*. Nature 263:521–523. https://doi.org/10.1038/263521a0

Hodková M, Okuda T (2019) Three kinds of regulatory signals for production of juvenile hormone in females of the linden bug, *Pyrrhocoris apterus*. J Insect Physiol 113:17–23. https://doi.org/10.1016/j.jinsphys.2019.01.002

Ikeda K, Daimon T, Shiomi K et al (2021) Involvement of the clock gene *period* in the photoperiodism of the silkmoth *Bombyx mori*. Zoolog Sci 38:523–530. https://doi.org/10.2108/zs210081

Ikeno T, Tanaka SI, Numata H, Goto SG (2010) Photoperiodic diapause under the control of circadian clock genes in an insect. BMC Biol 8:116. https://doi.org/10.1186/1741-7007-8-116

Ikeno T, Numata H, Goto SG (2011a) Circadian clock genes *period* and *cycle* regulate photoperiodic diapause in the bean bug *Riptortus pedestris* males. J Insect Physiol 57:935–938. https://doi.org/10.1016/j.jinsphys.2011.04.006

Ikeno T, Numata H, Goto SG (2011b) Photoperiodic response requires *mammalian-type cryptochrome* in the bean bug *Riptortus pedestris*. Biochem Biophys Res Commun 410:394–397. https://doi.org/10.1016/j.bbrc.2011.05.142

Ikeno T, Ishikawa K, Numata H, Goto SG (2013) Circadian clock gene *Clock* is involved in the photoperiodic response of the bean bug *Riptortus pedestris*. Physiol Entomol 38:157–162. https://doi.org/10.1111/phen.12013

Ikeno T, Numata H, Goto SG, Shiga S (2014) The involvement of the brain region containing pigment-dispersing factor-immunoreactive neurons in the photoperiodic response of the bean bug *Riptortus pedestris*. J Exp Biol 217:453–462. https://doi.org/10.1242/jeb.091801

Kamano S (1991) *Riptorus clavatus* (Thunberg) (Bean bug). In: Yushima T, Kamano S, Tamaki Y (eds) Rearing methods of insects. Japan Plant Protection Association, Tokyo, pp 46–49. (in Japanese)

Kang DS, Denlinger DL, Sim C (2014) Suppression of allatotropin simulates reproductive diapause in the mosquito *Culex pipiens*. J Insect Physiol 64:48–53. https://doi.org/10.1016/j.jinsphys.2014.03.005

Koide R, Xi J, Hamanaka Y, Shiga S (2021) Mapping PERIOD-immunoreactive cells with neurons relevant to photoperiodic response in the bean bug *Riptortus pedestris*. Cell Tissue Res 385:571–583. https://doi.org/10.1007/s00441-021-03451-6

Kubrak OI, Kučerová L, Theopold U, Nässel DR (2014) The sleeping beauty: How reproductive diapause affects hormone signaling, metabolism, immune response and somatic maintenance in *Drosophila melanogaster*. PLoS ONE 9:e113051. https://doi.org/10.1371/journal.pone.0113051

Kurogi Y, Mizuno Y, Imura E, Niwa R (2021) Neuroendocrine regulation of reproductive dormancy in the fruit fly *Drosophila melanogaster*: A review of juvenile hormone-dependent regulation. Front Ecol Evol 9:715029. https://doi.org/10.3389/fevo.2021.715029

Larrere M, Lavenseau L, Tasei J-N, Couillaud F (1993) Juvenile hormone biosynthesis and diapause termination in *Bombus terrestris*. Invertebr Reprod Dev 23:7–14. https://doi.org/10.1080/07924259.1993.9672288

Lee J, Kim C-H, Jang HA et al (2019) *Burkholderia* gut symbiont modulates titer of specific juvenile hormone in the bean bug *Riptortus pedestris*. Dev Comp Immunol 99:103399. https://doi.org/10.1016/j.dci.2019.103399

Li W, Huang ZY, Liu F et al (2013) Molecular cloning and characterization of juvenile hormone acid methyltransferase in the honey bee, *Apis mellifera*, and its differential expression during caste differentiation. PLoS ONE 8:e68544. https://doi.org/10.1371/journal.pone.0068544

Marchal E, Zhang J, Badisco L et al (2011) Final steps in juvenile hormone biosynthesis in the desert locust, *Schistocerca gregaria*. Insect Biochem Mol Biol 41:219–227. https://doi.org/10.1016/j.ibmb.2010.12.007

Matsumoto K, Numata H, Shiga S (2013) Role of the brain in photoperiodic regulation of juvenile hormone biosynthesis in the brown-winged green bug *Plautia stali*. J Insect Physiol 59:387–393. https://doi.org/10.1016/j.jinsphys.2013.01.007

Matsumoto K, Suetsugu Y, Tanaka Y et al (2017) Identification of allatostatins in the brown-winged green bug *Plautia stali*. J Insect Physiol 96:21–28. https://doi.org/10.1016/j.jinsphys.2016.10.005

Meuti ME, Stone M, Ikeno T, Denlinger DL (2015) Functional circadian clock genes are essential for the overwintering diapause of the Northern house mosquito, *Culex pipiens*. J Exp Biol 218:412–422. https://doi.org/10.1242/jeb.113233

Miki T, Shinohara T, Chafino S et al (2020) Photoperiod and temperature separately regulate nymphal development through JH and insulin/TOR signaling pathways in an insect. Proc Natl Acad Sci USA 117:5525–5531. https://doi.org/10.1073/pnas.1922747117

Minakuchi C, Namiki T, Yoshiyama M, Shinoda T (2008) RNAi-mediated knockdown of *juvenile hormone acid O-methyltransferase* gene causes precocious metamorphosis in the red flour beetle *Tribolium castaneum*. FEBS J 275:2919–2931. https://doi.org/10.1111/j.1742-4658.2008.06428.x

Miura K, Shinoda T, Yura M et al (1998) Two hexameric cyanoprotein subunits from an insect, *Riptortus clavatus*. Sequence, phylogeny and developmental and juvenile hormone regulation. Eur J Biochem 258:929–940. https://doi.org/10.1046/j.1432-1327.1998.2580929.x

Mizoguchi A, Okamoto N (2013) Insulin-like and IGF-like peptides in the silkmoth *Bombyx mori*: discovery, structure, secretion, and function. Front Physiol 4:217. https://doi.org/10.3389/fphys.2013.00217

Mizoguchi A, Ishizaki H, Nagasawa H et al (1987) A monoclonal antibody against a synthetic fragment of bombyxin (4K-prothoracicotropic hormone) from the silkmoth, *Bombyx mori*: characterization and immunohistochemistry. Mol Cell Endocrinol 51:227–235. https://doi.org/10.1016/0303-7207(87)90032-3

Morita A, Numata H (1997) Role of the neuroendocrine complex in the control of adult diapause in the bean bug, *Riptortus clavatus*. Arch Insect Biochem Physiol 35:347–355. https://doi.org/10.1002/(SICI)1520-6327(199705)35:3%3c347::AID-ARCH8%3e3.0.CO;2-Q

Morita A, Soga K, Hoson T et al (1999) Changes in mechanical properties of the cuticle and lipid accumulation in relation to adult

diapause in the bean bug, *Riptortus clavatus*. J Insect Physiol 45:241–247. https://doi.org/10.1016/S0022-1910(98)00119-X

Mukai A, Goto SG (2016) The clock gene *period* is essential for the photoperiodic response in the jewel wasp *Nasonia vitripennis* (Hymenoptera: Pteromalidae). Appl Entomol Zool 51:185–194. https://doi.org/10.1007/s13355-015-0384-1

Nagy D, Cusumano P, Andreatta G et al (2019) Peptidergic signaling from clock neurons regulates reproductive dormancy in *Drosophila melanogaster*. PLoS Genet 15:e1008158. https://doi.org/10.1371/journal.pgen.1008158

Nässel DR, Broeck JV (2015) Insulin/IGF signaling in *Drosophila* and other insects: factors that regulate production, release and post-release action of the insulin-like peptides. Cell Mol Life Sci 73:271–290. https://doi.org/10.1007/s00018-015-2063-3

Nelson RJ, Denlinger DL, Somers DE (2009) Photoperiodism. Oxford University Press, New York

Niwa R, Niimi T, Honda N et al (2008) Juvenile hormone acid O-methyltransferase in *Drosophila melanogaster*. Insect Biochem Mol Biol 38:714–720. https://doi.org/10.1016/j.ibmb.2008.04.003

Nouzova M, Edwards MJ, Michalkova V et al (2021) Epoxidation of juvenile hormone was a key innovation improving insect reproductive fitness. Proc Natl Acad Sci USA 118:e2109381118. https://doi.org/10.1073/pnas.2109381118

Numata H, Hidaka T (1982) Photoperiodic control of adult diapause in the bean bug, *Riptortus clavatus* Thunberg (Heteroptera : Coreidae). I. Reversible induction and termination of diapause. Appl Entomol Zool 17:530–538. https://doi.org/10.1303/aez.17.530

Numata H, Miyazaki Y, Ikeno T (2015) Common features in diverse insect clocks. Zool Lett 1:10. https://doi.org/10.1186/s40851-014-0003-y

Ojima N, Hara Y, Ito H, Yamamoto D (2018) Genetic dissection of stress-induced reproductive arrest in *Drosophila melanogaster* females. PLoS Genet 14:e1007434. https://doi.org/10.1371/journal.pgen.1007434

Okamoto N, Yamanaka N (2015) Nutrition-dependent control of insect development by insulin-like peptides. Curr Opin Insect Sci 11:21–30. https://doi.org/10.1016/j.cois.2015.08.001

Okuda T, Tanaka S, Kotaki T, Ferenz H-J (1996) Role of the corpora allata and juvenile hormone in the control of imaginal diapause and reproduction in three species of locusts. J Insect Physiol 42:943–951. https://doi.org/10.1016/0022-1910(96)00055-8

Patke A, Young MW, Axelrod S (2020) Molecular mechanisms and physiological importance of circadian rhythms. Nat Rev Mol Cell Biol 21:67–84. https://doi.org/10.1038/s41580-019-0179-2

Peffers C, Meuti ME (2022) Characterizing the relative abundance of circadian transcription factors in diapausing and nondiapausing Northern house mosquitoes. J Insect Physiol 140:104404. https://doi.org/10.1016/j.jinsphys.2022.104404

Poras M (1982) Le Contrôle endocrinien de la diapause imaginale des femelles de *Tetrix undulata* (Sowerby, 1806) (Orthoptere, Tetrigidae). Gen Comp Endocrinol 46:200–210. https://doi.org/10.1016/0016-6480(82)90202-7

Rankin MA, Riddiford LM (1978) Significance of haemolymph juvenile hormone titer changes in timing of migration and reproduction in adult *Oncopeltus fasciatus*. J Insect Physiol 24:31–38. https://doi.org/10.1016/0022-1910(78)90008-2

Readio J, Chen M-H, Meola R (1999) Juvenile hormone biosynthesis in diapausing and nondiapausing *Culex pipiens* (Diptera: Culicidae). J Med Entomol 36:355–360. https://doi.org/10.1093/jmedent/36.3.355

Riehle MA, Fan Y, Cao C, Brown MR (2006) Molecular characterization of insulin-like peptides in the yellow fever mosquito, *Aedes aegypti*: expression, cellular localization, and phylogeny. Peptides 27:2547–2560. https://doi.org/10.1016/j.peptides.2006.07.016

Schiesari L, Andreatta G, Kyriacou CP et al (2016) The insulin-like proteins dILPs-2/5 determine diapause inducibility in *Drosophila*. PLoS ONE 11:e0163680. https://doi.org/10.1371/journal.pone.0163680

Sheng Z, Xu J, Bai H et al (2011) Juvenile hormone regulates vitellogenin gene expression through insulin-like peptide signaling pathway in the red flour beetle, *Tribolium castaneum*. J Biol Chem 286:41924–41936. https://doi.org/10.1074/jbc.M111.269845

Shiga S, Numata H (2000) The role of neurosecretory neurons in the pars intercerebralis and pars lateralis in reproductive diapause of the blowfly, *Protophormia terraenovae*. Naturwissenschaften 87:125–128. https://doi.org/10.1007/s001140050689

Shimokawa K, Numata H, Shiga S (2008) Neurons important for the photoperiodic control of diapause in the bean bug, *Riptortus pedestris*. J Comp Physiol A 194:751–762. https://doi.org/10.1007/s00359-008-0346-y

Shimokawa K, Numata H, Shiga S (2014) Pars intercerebralis promotes oviposition in the bean bug, *Riptortus pedestris* (Heteroptera: Alydidae). Appl Entomol Zool 49:525–528. https://doi.org/10.1007/s13355-014-0281-z

Shinoda T, Itoyama K (2003) Juvenile hormone acid methyltransferase: A key regulatory enzyme for insect metamorphosis. Proc Natl Acad Sci USA 100:11986–11991. https://doi.org/10.1073/pnas.2134232100

Sim C, Denlinger DL (2008) Insulin signaling and FOXO regulate the overwintering diapause of the mosquito *Culex pipiens*. Proc Natl Acad Sci USA 105:6777–6781. https://doi.org/10.1073/pnas.0802067105

Sim C, Denlinger DL (2009) A shut-down in expression of an insulin-like peptide, ILP-1, halts ovarian maturation during the overwintering diapause of the mosquito *Culex pipiens*. Insect Mol Biol 18:325–332. https://doi.org/10.1111/j.1365-2583.2009.00872.x

Sim C, Denlinger DL (2013a) Insulin signaling and the regulation of insect diapause. Front Physiol 4:189. https://doi.org/10.3389/fphys.2013.00189

Sim C, Denlinger DL (2013b) Juvenile hormone III suppresses forkhead of transcription factor in the fat body and reduces fat accumulation in the diapausing mosquito, *Culex pipiens*. Insect Mol Biol 22:1–11. https://doi.org/10.1111/j.1365-2583.2012.01166.x

Sim C, Kang DS, Kim S et al (2015) Identification of FOXO targets that generate diverse features of the diapause phenotype in the mosquito *Culex pipiens*. Proc Natl Acad Sci USA 112:3811–3816. https://doi.org/10.1073/pnas.1502751112

Steel CGH, Vafopoulou X (2006) Circadian orchestration of developmental hormones in the insect, *Rhodnius prolixus*. Comp Biochem Physiol 144:351–364. https://doi.org/10.1016/j.cbpa.2006.02.018

Tamai T, Shiga S, Goto SG (2019) Roles of the circadian clock and endocrine regulator in the photoperiodic response of the brown-winged green bug *Plautia stali*. Physiol Entomol 44:43–52. https://doi.org/10.1111/phen.12274

Tauber MJ, Tauber CA, Masaki S (1986) Seasonal Adaptations of Insects. Oxford University Press, New York

Thompson JD, Higgins DG, Gibson TJ (1994) CLUSTAL W: improving the sensitivity of progressive multiple sequence alignment through sequence weighting, position-specific gap penalties and weight matrix choice. Nucleic Acids Res 22:4673–4680. https://doi.org/10.1093/nar/22.22.4673

Tian Z, Guo S, Li J-X et al (2021) Juvenile hormone biosynthetic genes are critical for regulating reproductive diapause in the cabbage beetle. Insect Biochem Mol Biol 139:103654. https://doi.org/10.1016/j.ibmb.2021.103654

Tomioka K, Matsumoto A (2019) The circadian system in insects: Cellular, molecular, and functional organization. In: Jurenka R (Ed) Advances in Insect Physiology, vol 56. Academic Press, Oxford, UK, pp 73–115. https://doi.org/10.1016/bs.aiip.2019.01.001

Vafopoulou X, Steel CGH (2012) Insulin-like and testis ecdysiotropin neuropeptides are regulated by the circadian timing system in the brain during larval-adult development in the insect *Rhodnius*

prolixus (Hemiptera). Gen Comp Endocrinol 179:277–288. https://doi.org/10.1016/j.ygcen.2012.08.018

Vafopoulou X, Steel CGH (2014) Synergistic induction of the clock protein PERIOD by insulin-like peptide and prothoracicotropic hormone in *Rhodnius prolixus* (Hemiptera): implications for convergence of hormone signaling pathways. Front Physiol 5:41. https://doi.org/10.3389/fphys.2014.00041

Xu H-J, Xue J, Lu B et al (2015) Two insulin receptors determine alternative wing morphs in planthoppers. Nature 519:464–467. https://doi.org/10.1038/nature14286

Zhan S, Merlin C, Boore JL, Reppert SM (2011) The monarch butterfly genome yields insights into long-distance migration. Cell 147:1171–1185. https://doi.org/10.1016/j.cell.2011.09.052

Zhang C, Daubnerova I, Jang Y-H et al (2021) The neuropeptide allatostatin C from clock-associated DN1p neurons generates the circadian rhythm for oogenesis. Proc Natl Acad Sci USA 118:e2016878118. https://doi.org/10.1073/pnas.2016878118

Zhu L, Tian Z, Guo S et al (2019) Circadian clock genes link photoperiodic signals to lipid accumulation during diapause preparation in the diapause-destined female cabbage beetles *Colaphellus bowringi*. Insect Biochem Mol Biol 104:1–10. https://doi.org/10.1016/j.ibmb.2018.11.001